BOLETIN DE LA SOCIEDAD ESPAÑOLA DE
Cerámica y Vidrio
www.elsevier.es/bsecv

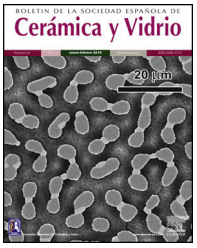

Mullite fabrication from natural kaolin and aluminium slag

Fouzia Chargui[a,b], *Mohamed Hamidouche*[a,b,*], *Hocine Belhouchet*[c,d], *Yves Jorand*[e], *Rachida Doufnoune*[a,f], *Gilbert Fantozzi*[e]

[a] *Emergent Materials Research Unit, Setif 1 University, 19000 Setif, Algeria*
[b] *Optical and Precision Mechanical Institute, Setif 1 University, 19000 Setif, Algeria*
[c] *Non-metallic Materials Laboratory, Optical and Precision Mechanical Institute, Setif 1 University, 19000 Setif, Algeria*
[d] *Physical Department, Faculty of Science, Mohamed Boudiaf M'sila University, 28000 M'Sila, Algeria*
[e] *Lyon University, INSA-Lyon, MATEIS Laboratory CNRS-UMR 5510, 69621 Villeurbanne, France*
[f] *Process Engineering Department, Faculty of Technology, Setif 1 University, 19000 Setif, Algeria*

ARTICLE INFO

Article history:
Received 4 August 2017
Accepted 10 January 2018
Available online 18 February 2018

Keywords:
Mullite
Kaolin
Aluminum slag
Phase transformation

ABSTRACT

The structural transformations of kaolin–aluminium slag mixtures during heating were studied using differential thermal analysis (DTA), thermal gravimetric analysis (TGA), Fourier transform infrared (FTIR) spectroscopy, X-ray diffraction analysis (XRD) and scanning electron microscopy (SEM). The amount of formed mullite increases with the firing temperature. At 1500 °C, the mullitization of the mixture is almost complete. The morphology of the formed mullite is bimodal (primary and secondary phases). The primary mullite, formed from processing of kaolin by the gradual collapse of metakaolin from 990 °C, has a shape of elongated crystals. The other hand, the secondary mullite formed by solution-precipitation from the glass phase in the presence of alumina particles has a shape of acicular grains.

Producción de mullita a partir de caolín natural y escoria de aluminio

Palabras clave:
Mullita
Caolín
Escoria de aluminio
Transformación de fase

RESUMEN

Se estudiaron las transformaciones estructurales de las mezclas de caolín y escoria de aluminio durante el calentamiento mediante análisis térmico diferencial (ATD), análisis termogravimétrico (ATG), espectroscopía infrarroja por transformada de Fourier (EITF), análisis por difracción de rayos X (XRD, por sus siglas en inglés) y microscopia electrónica de barrido (MEB). La cantidad de mullita creada aumenta con la temperatura de cocción. A 1.500 °C, la mullitización de la mezcla es casi completa. La morfología de la mullita creada es bimodal (fases primaria y secundaria). La mullita primaria, creada a partir del

* *Corresponding author.*
E-mail addresses: mhamidouche@univ-setif.dz, mhamidouche@yahoo.fr (M. Hamidouche).
https://doi.org/10.1016/j.bsecv.2018.01.001

procesamiento del caolín por la paulatina desintegración del metacaolín a partir de 990 °C, tiene una forma de cristales alargados. Además, la mullita secundaria creada por disolución-precipitación a partir de la fase de vidrio en presencia de partículas de alúmina tiene una forma de granos aciculares.

Introduction

Mullite, whose chemical composition is found between $3Al_2O_3$-$2SiO_2$ and $2Al_2O_3$-SiO_2, is one of the most studied and used ceramics. Its applications are very diverse and cover from refractory field to technical applications [1–3]. In air and under atmospheric pressure, it is thermally and chemically stable from room temperature to melting one [4]. It has very good thermo-mechanical properties, which allows us to use it as structural elements such as thermal engines. Indeed, sensitivity to creep is very limited [5]. Its thermal expansion coefficient is relatively low leading to a good thermal shock resistance [6].

We use different precursors and methods to synthesize mullite. We manufacture it through several reactive processes at different temperatures [7]. Each fabrication method has specific features depending on the wanted application and product performance. Solid phase reaction oxides alumina-silica mixtures at high temperature, generally above 1400 °C [8], can lead to mullite formation. By sol–gel methods [9], or co-precipitation of mixtures of salts in solution based on silicon and aluminium, we synthesize low-temperature mullite [11]. On the contrary, when the precursors are natural alumino-silicate clays, we form the mullite by thermal processes lower than 1300 °C [12].

Kaolin, whose main constituent is kaolinite ($Al_2Si_2O_5(OH)_4$), undergoes successive structural and microstructural transformations during its firing [13]. The decomposition of kaolinite in metakaolinite takes place between 400 °C and 630 °C. The gradual collapse of metakaolin promotes the formation of nanoscale crystals of mullite, in addition to formation of free amorphous silica. At 1200 °C, the crystallization of cristobalite is triggered from amorphous silica, and a considerable amount of mullite crystals is developed [14]. The last transformation step is the verification of cristobalite, which occurs at a temperature generally above 1400 °C. The presence of some impurities, such as CaO, Na_2O and K_2O, in the initial kaolin favours vitrification of cristobalite at lower temperatures. To obtain a secondary mullite, this silica glass can be 'mullitized' by adding alumina, aluminium hydroxides or aluminium slag [15]. Secondary mullite is different to the primary one by the morphology and grain size [16]. Primary mullite forms needles, due to the presence of the vitreous phase [17]. While secondary mullite is in the form of aggregates of needle-like small grains [18], we form it by a solution-precipitation of the glass phase in contact with the particles of alumina. According to Pascual et al., addition of 1–3 wt% of MgO to the kaolin-alumina mixture promotes grain growth of primary and secondary mullite, and the addition of 1–5% Y_2O_3 inhibits grain growth of the secondary mullite [19]. We detect no difference in the X-ray diffraction spectra of the two mullites. However, we observe differences between infrared absorption spectra.

The aim of the present work is the mullitization of two types of Algerian kaolin by adding aluminium slag. We have sintered stoichiometric mixtures at temperatures between 1000 °C and 1500 °C for 2 h. In order to understand microstructural transformations and chemical reactions, we performed differential thermal analysis coupled with thermal gravimetric analysis (DTA/TGA). We have analysed, by X-ray diffraction (XRD), the phase transformations during the various thermal treatments. We determined the morphology of mullite by scanning electron microscopy (SEM). We studied the chemical bonds of the phases formed during the firing of aluminium kaolin-slag mixtures at different temperatures by Fourier transform infrared (FTIR) spectroscopy.

Experimental procedure

We have used two natural kaolin extracted from two various sites of Djebel Debbagh near Guelma (North-East of Algeria). The amount of alumina in their composition and colour differentiate the two kaolin. The first composition noted DD1 is white coloured where as the second one (DD3) in greyish coloured. The difference in their colours is due to the kind of their containing impurities.

Their absolute densities, measured with a helium pycnometer apparatus are respectively 2.63 g/cm^3 for DD1 and 2.61 g/cm^3 for DD3. The used aluminium slag, waste of aluminium industry, is provided by ALGAL company (Algeria). It is white coloured and composed by 87% (in mass) of alumina, its absolute density is about 4.03 g/cm^3.

Tabla 1 represents the chemical compositions of respectively both kaolin and aluminium slag.

To obtain mullite we prepared, with a stoichiometric composition, two mixtures of DD1 and DD3 with aluminium slag, they are respectively noted MDD1 and MDD3.

We milled the mixtures with a planetary ball milling apparatus during 5 h; with a report powder/balls equal to (50/200) g in 80 ml water.

We dried the mixtures at 110 °C and then crushed and sieved to 45 μm meshes. The samples were uniaxial pressed at 100 MPa for obtaining bars shaped (40 mm × 10 mm × 10 mm), after that they were heated up to 600 °C at a rate of 1 °C/min for 1 h to avoid cracking. Then we sintered the samples between 1000 °C and 1500 °C for 2 h, with a heating rate of 5 °C/min. We subjected powders mixtures MDD1 and MDD3 to differential thermal analysis (DTA) and thermo gravimetric analysis (TGA) using Setaram Setsys 16/18 simultaneous TG/DTA analyzer with α-alumina as the reference material. We conducted the test between the room temperature and

Tabla 1 – Chemical compositions of kaolin and aluminium slag.

Oxides	SiO_2	Al_2O_3	Fe_2O_3	CaO	MgO	TiO_2	Na_2O	K_2O	Fire loss (%)
Kaolin DD1	44.9	37.49	0.12	0.26	0.13	0.1	0.19	0.01	17%
Kaolin DD3	43	39.9	1.9	0.20	0	0	0.06	0.10	15%
Aluminium slag	2.5	87	0.15	0.12	0.21	0.2	0.2	0.1	9.52%

1400 °C in air atmosphere with a heating rate of 5 °C/min. We have used a helium pycnometer (AccuPyc II1340) to determine the absolute density of calcined kaolin, aluminium slag and there mixtures at different temperatures. We studied the evolution of the crystalline phases, according to the temperatures treatment, by the X-rays diffraction (Brücker AXS). We calculated the rate of mullite formation, as a function of thermal treatment, using the internal standard method and the I/I_{cor} relation presented in the JCPDS standard cards.

We analysed, by Fourier transform infrared (FTIR) spectroscopy, the presence of specific atomic groupings and the characteristic vibrations of the chemical bands. We made the tests on translucent pastilles obtained by the mixture of 99% mg from the material to be analysed crushed well with 1% mg of Kbr by means of a device of type Perkin-Elmes700. The samples were polished and thermally etched to observe the microstructure by using a scanning electron microscope (SEM) (Zeiss SUPRA 55VP type).

Results and discussion

The X-ray diffraction analysis spectra (Fig. 1) revealed that both the used kaolins contain essentially kaolinite (Index JCPDS 80-0886) and halloysite (JCPDS 29-1489).

The aluminium slag is totally transformed into α-alumina after a thermal treatment at 1400 °C where its absolute density is equal to 3.41 g/cm^3 (Fig. 2).

The observation of kaolin powders by SEM (Fig. 3) revealed a structure composed of agglomerates of leaves lengthened and oriented in all directions. These cases, randomly entangled, have favoured an important porosity.

The observation of aluminium slag by SEM showed a structure composed of agglomerates of spherical grains.

In Fig. 4, we presented differential thermal analyses curves of DD1, DD3 kaolin and aluminium slag. The DTA/TG curves of both kaolin show the presence of two endothermic peaks.

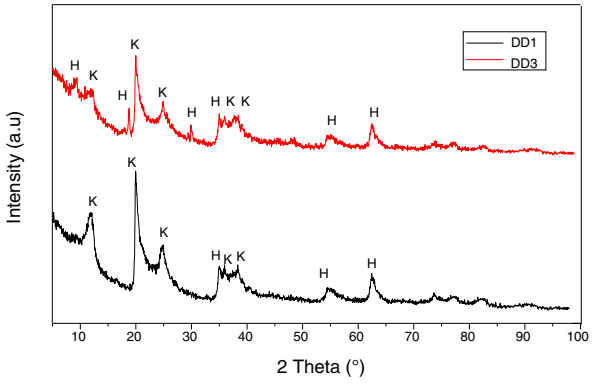

Fig. 1 – XRD spectra of the used natural kaolin, K: kaolinite; H: halloysite.

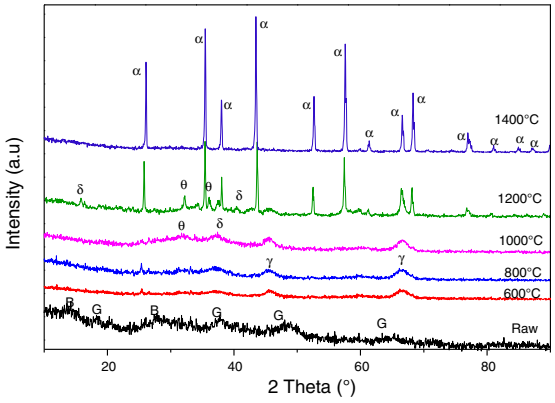

Fig. 2 – XRD spectra of the aluminium slag of the thermal treatment at different temperatures (α: alpha alumina; γ: gamma alumina; θ: theta alumina; δ: delta alumina; B: boehmite; G: gibbsite).

The first one is very intense, has a maximum located at 86 °C, it is due to the departure of the surface water. The second one appeared at 532 °C. It is related to the departure of constitution water (dehydration of kaolin to form metakaolin) and associated to a mass loss of (12.5% for DD3 and 12.75% for DD1), between 400 °C and 600 °C. Furthermore, the DTA curves present an exothermic peak of low intensity at 988 °C; corresponding to the mullite crystallization formed from the kaolinite transformation.

The DTA curve of the aluminium slag shows an endothermic peak of a very marked intensity towards 119 °C, linked to moisture water. Endothermic peak at 270 °C introduces the dehydration of the tri-hydrate oxide to mono-hydroxide (boehmite). We noticed a mass loss of 6.5%, with these transformations. Therefore, in addition to these endothermic peaks, the TDA curve presents other exothermic effects. We attributed the first exothermic peak, which appears between 400 °C and 600 °C centred at 449 °C, to a rapid transition reaction triggered by the beginning of changes in the slag crystal structure, which is accompanied by a loss mass of 2%. Raw aluminium slag is globally amorphous with the presence of gibbsite and boehmite (Fig. 2). The gibbsite–boehmite phase transformation takes place around 270 °C (see DTA curve in Fig. 4). Between 400 °C and 550 °C, boehmite is transformed into gamma alumina. This transition alumina then leads to alumina delta and theta between 800 °C and 1200 °C. Above 1200 °C, the formation of the stable alpha-alumina phase takes place. These transformations of hydrated alumina phases to transitions alumina and then to α-alumina have been detailed in our previous works [20–24].

We represented in Fig. 5 the evolution of the crystalline structure for the two kaolin using XRD. From 600 °C to 800 °C, the structure is amorphous for the two kaolins DD1 and DD3.

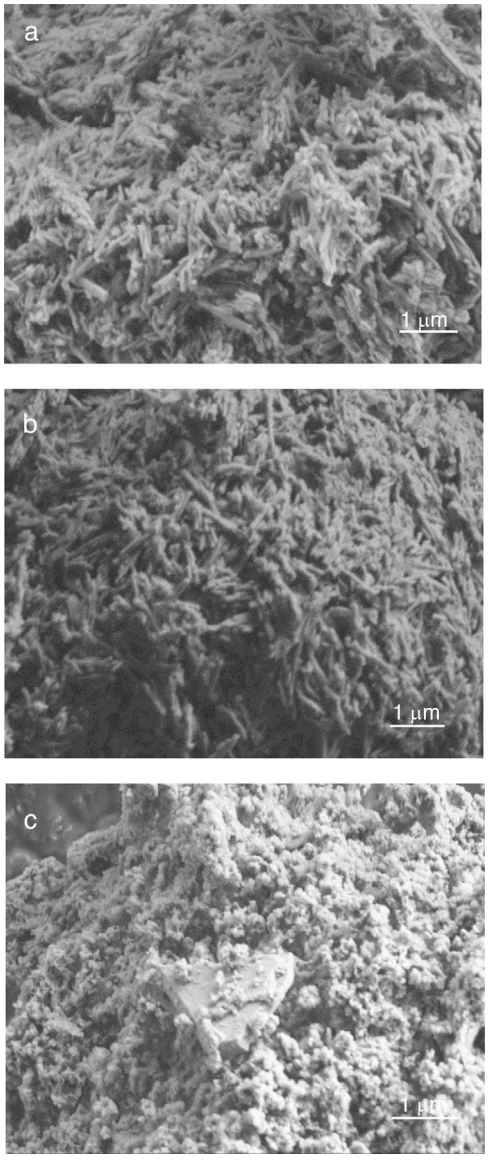

Fig. 3 – Microstructure of kaolin and aluminium slag used; (a) DD1, (b) DD3 and (c) aluminium slag.

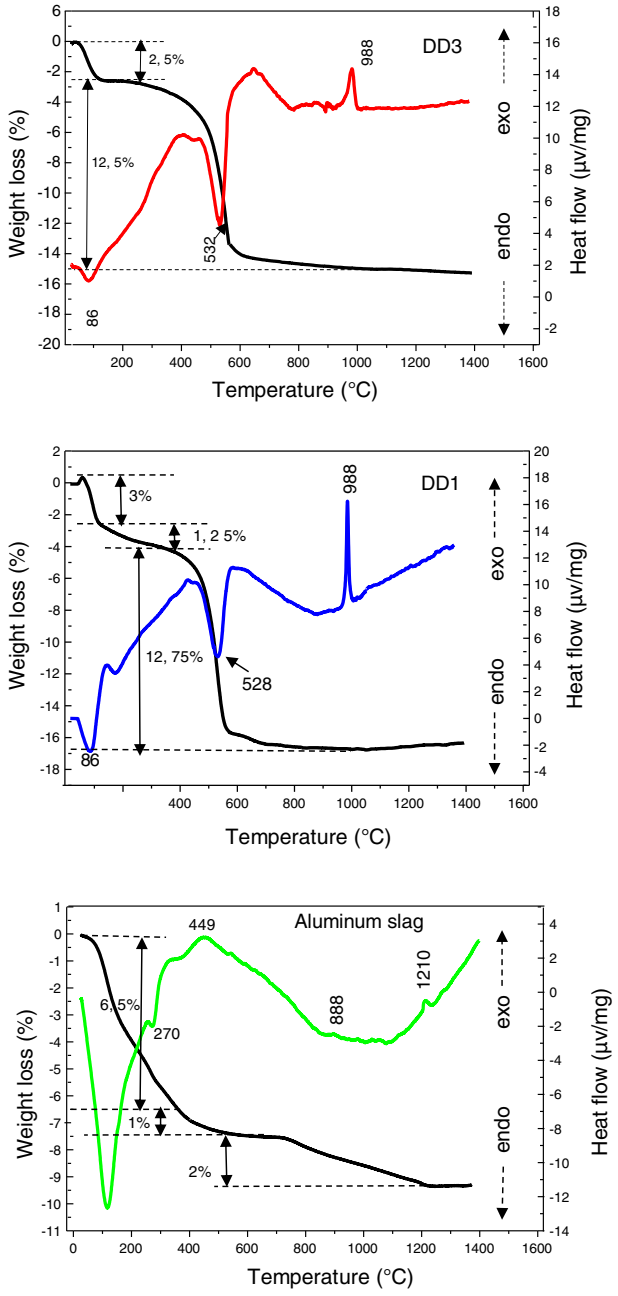

Fig. 4 – Differential thermal analysis and thermo gravimetric behaviour of kaolin DD3, DD1 and aluminium slag.

In the case of these kaolins, the formation of mullite begins at 1000 °C. At 1200 °C, the peaks of low intensities correspond to the germination of the mullite for DD1.

The mullite phase becomes important in the case of DD3 kaolin beyond 1200 °C. Also that, starting from 1200 °C, the excess of silica leads to the crystallization of the cristobalite. At 1500 °C, we noticed for both kaolins, the increases of the peaks intensities caused by the increase of mullite quantity. On the other hand, at this temperature, the peak of the cristobalite disappears because of its transformation into vitreous phase.

The DTA/TG curves of MDD1 and MDD 3 mixtures (Fig. 6) show two endothermic peaks. The first one is very intense, has a maximum located at 100 °C, it is caused by the departure of the surface water. This last is associated to a mass loss between 20 °C and 400 °C. The second one appeared at 537 °C for MDD3 and at 532 °C for MDD1. It corresponds to the departure of constitution water (dehydration of kaolin), associated with a low mass loss between 375 °C and 600 °C. Besides, these two endothermic peaks, the DTA curve presents other exothermic effects of low intensities, which are not associated with any loss of mass. According to Gonon et al. [15], the first exothermic peak in neighbourhood of 1000 °C corresponds to the crystallization of the mullite from metakaolin. The second less intense exothermic peak, observed in the neighbourhood of 1194 °C for the MDD3 and 1220 °C for the MDD1, is associated to the formation of the secondary mullite by reaction of the alumina resulting from aluminium slag with the excess of silica of the kaolin [20,25]. For the clay; the phase, which

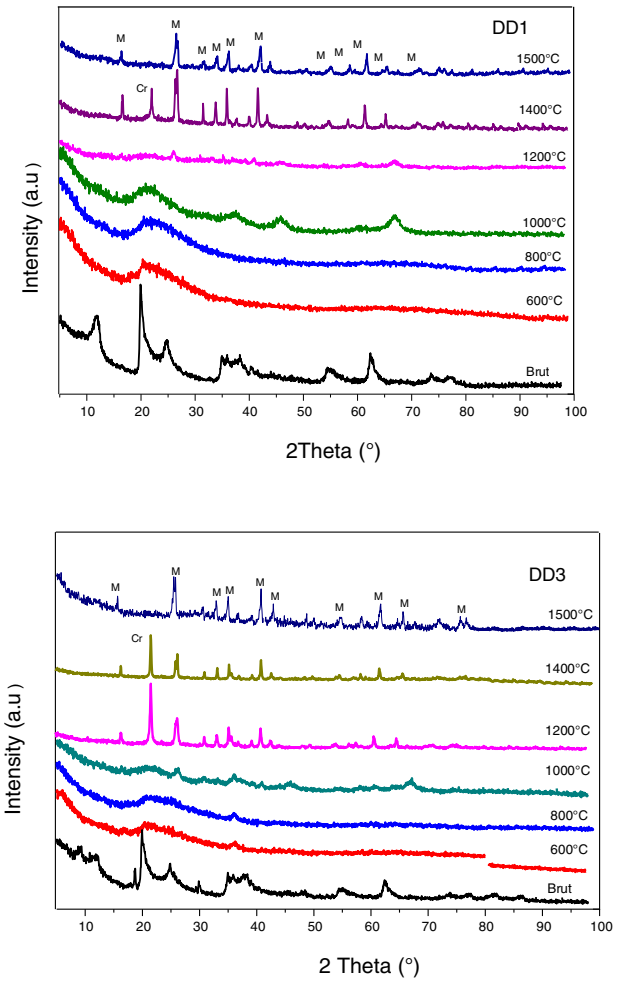

Fig. 5 – XRD of the kaolin treated at different temperatures. M: mullite; Cr: cristobalite.

crystallized from 850 °C can melt [26]. Its melting occurs between 1100 °C and 1300 °C [27]. Increasing iron content into the various starting kaolins leads to the secondary mullite formation towards lower temperatures [27].

Fig. 7 represents the XRD diagrams of MDD1 and MDD3 mixtures fired at different temperatures.

At 1000 °C, the beginning of the crystallization of the primary mullite formed from the kaolin. At the same temperature, we observed a peak relating to the formation of γ-alumina at $2\theta = 65°$. The XRD curves of samples fired at 1100 °C and at 1200 °C show the same formed crystalline phases, namely the alumina γ and the primary mullite. We noticed the non-appearance of the cristobalite peak, formed at this temperature in the case of the kaolin DD3 alone. We explained this, by the formation of the secondary mullite due to the reaction of the γ-alumina from the slag with the excess of silica from the kaolin before the crystallization of the latter into cristobalite.

The firing of MDD1 and MDD3 mixtures at 1300 °C and 1400 °C leads to the acceleration of the formation of the secondary mullite. At 1500 °C, practically almost complete mullite formation of mixtures. The present impurities in the precursors (slag and kaolin) with one part of the silica form a glassy

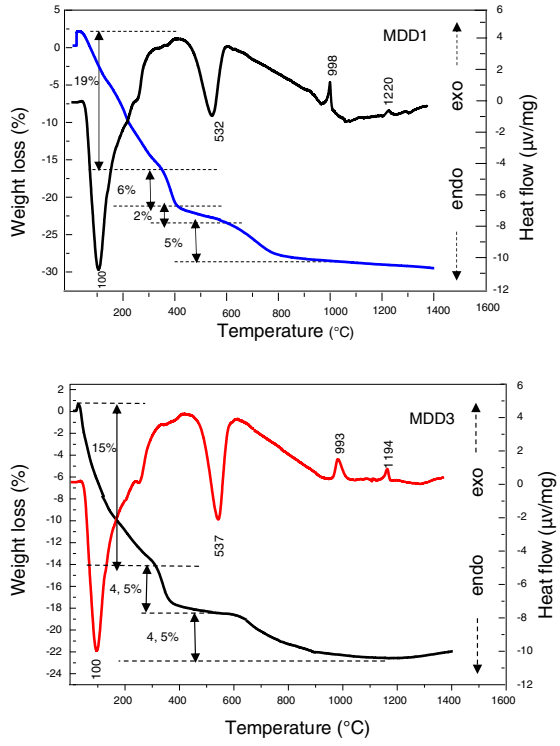

Fig. 6 – DTA/TG of mixtures MDD1and MDD3.

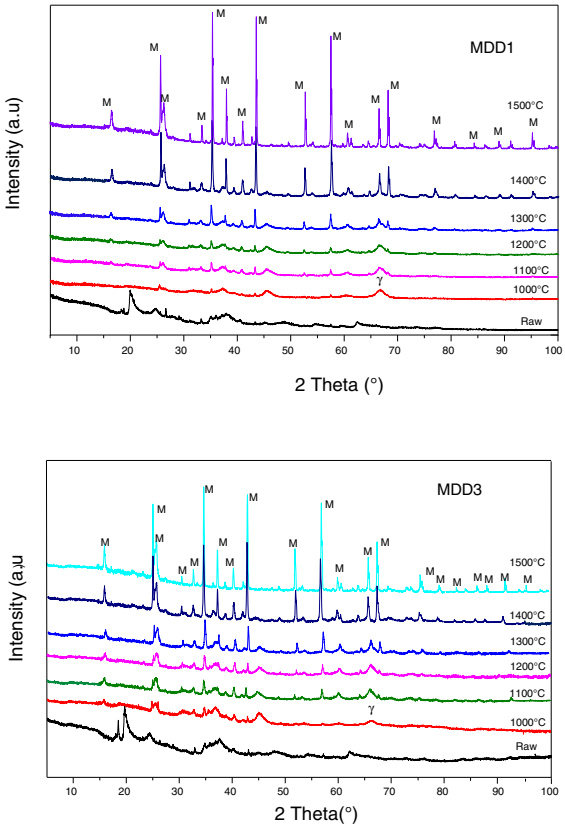

Fig. 7 – Diffractograms of MDD1 and MDD3 mixtures at different stages of the thermal treatment (M: mullite; γ: gamma alumina).

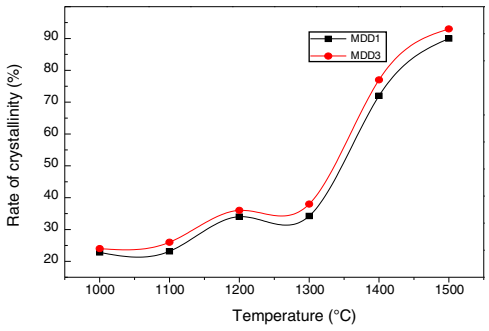

Fig. 8 – Variation of the crystallinity rate of MDD1 and MDD3 mixtures as a function of temperature treatment.

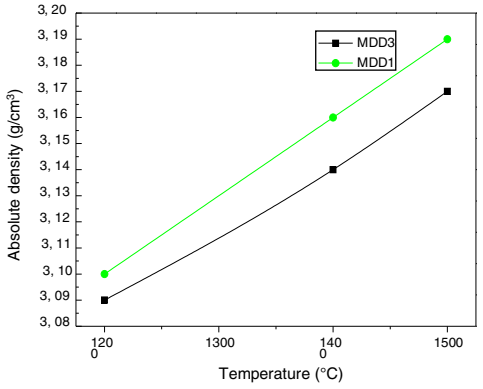

Fig. 9 – Evolution of the absolute density of MDD1 and MDD3 mixtures a function of the temperature.

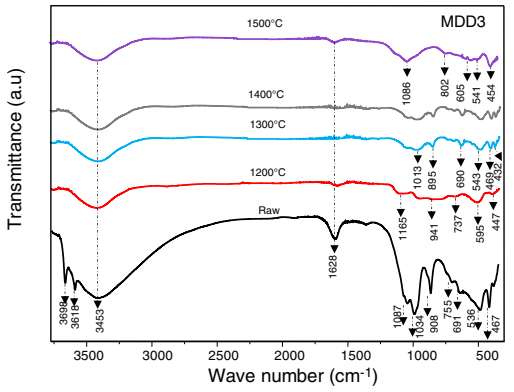

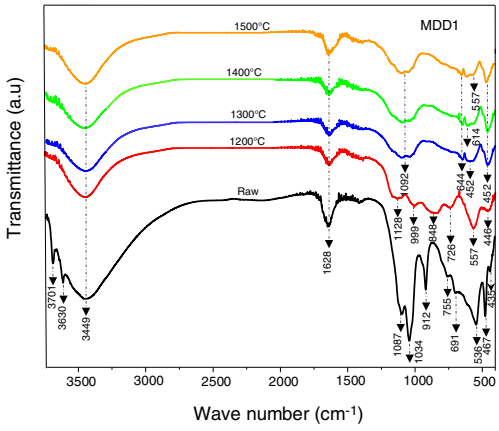

Fig. 10 – FTIR spectra of mixtures treated at different temperatures.

phase. The difference between the DRX spectra of the mixtures MDD1 and MDD3 resides in the quantity of mullite formed.

According to the calculation of the intensities of rays characterizing the mullite (Fig. 8), the crystallization rate of the mullite phase increases with the increase in the temperature of the heat treatment.

This rate reaches practically 94% for the mixture MDD1 and 89% for the mixture MDD3 for samples firing during 2 h at 1500 °C. We explained this difference between both mixtures by the high rate of SiO_2 in DD1 kaolin.

The quantity of the formed mullite is important in MDD1 mixture, of the fact that the high content of silica in its raw material (DD1). This necessity to an addition of aluminium slag is more important.

We measured absolute densities of mixtures (slag + kaolin), cured between 1200 °C and 1600 °C, by helium pycnometry. We gathered the results in Fig. 9. More the firing temperature increase, the absolute densities of mixtures also increase. At 1600 °C, they almost reach the theoretical value of the mullite density (3.17 g/cm^3).

Fig. 10 shows FTIR of MDD1 and MDD3 mixtures cured at different temperatures. In its natural state; in the range 4000–3000 cm^{-1} the spectra are characterized by two bands located at 3701 cm^{-1} and 3630 cm^{-1}, and a wide band centred at 3449 cm^{-1} for MDD1, and for MDD3 bands are respectively located at 3698 cm^{-1}, 3618 cm^{-1} and 3453 cm^{-1}, these bands are due to stretching vibration hydroxyls.

We assigned the bands located at 3701 cm^{-1} and 3698 cm^{-1} to the hydroxyls of the edges of leaves. Bands situated at 3630 cm^{-1}and 3618 cm^{-1} are for the hydroxyls of surface of the layer octahedral in interaction with basic oxygen of the tetrahedral adjacent layer. Finally, the bands at 3449 cm^{-1} and 3453 cm^{-1} are caused by the internal hydroxyls linked to the aluminium.

The bands that appeared at 1087 cm^{-1} and 1034 cm^{-1} was assigned to Si—O—Si stretching vibration. We attributed the bands at 912 cm^{-1} and 908 cm^{-1} for MDD1 and MDD3 respectively to vibrations of links Al—OH.

Si—O—Al^{VI} [12] and Si—O—Al^{IV} stretching vibrations are respectively characterized by bands at 536 cm^{-1} and 755 cm^{-1}.

We observed the band associated with Al—O—Al stretching for the two mixtures at 691 cm^{-1} [12]. On the other hand, the deformation of links Si—O is characterized by the presence of bands at 467 cm^{-1} and 435 cm^{-1}.

For a thermal treatment of MDD1 at 1200 °C, bands located respectively at 1087 cm^{-1} and 1134 cm^{-1} are transformed at a broader band constituted by two bands: the first one is centred at 1128 cm^{-1} and the second towards 999 cm^{-1}.

The bands located towards 755 cm^{-1} and 691 cm^{-1} are transformed in two wide bands. The first one indicates the formation of spinel Si—Al and the second indicates the crystallization of Al_2O_3 [10].

In addition, both the characteristic bands corresponding to Si—O stretching vibration are transformed to the single band of weak intensity centred at 446 cm^{-1}, which explains the decrease of the quantity of SiO_2.

The appearance of a wide band in the region 920–770 cm^{-1} centred towards 848 cm^{-1} assigned to Al—OH stretching vibration, is attributed to the crystallization of the secondary mullite [13].

On the other hand, the spectrum of mixture MDD3 at 1200 °C shows the appearance of a wide band in the region 1200–600 cm^{-1} centred respectively at 1165, 941 and 737 cm^{-1}, compared with the spectrum of MDD1. This wide band explains the training of a more important quantity of mullite.

For a treatment at 1300 °C, the band corresponding to the training of the mullite has become wider. This wide band is composed of two bands centred respectively towards 1104 and 1028 cm^{-1}, what can be explained by the training of addition al links of Si—O—Al in crystals of mullite.

Also, the wide band located at 848 cm^{-1} for the MDD1 mixture is replaced by a wide shoulder, and the spectrum of mixture MDD3 show the appearance of two new bands, one located at 895 cm^{-1} and the other at 690 cm^{-1}, and a less intense shoulder than that observed in the MDD1 spectrum. The thermal treatment at 1500 °C leads to the increase of the intensity of the band located at 1013 cm^{-1}.

The SEM results reveal that the morphology of microstructures of MDD1 and MDD3 does not present a significant difference between both mixtures after fired at 1400 °C during 2 h (Figs. 11 and 12).

We observed the existences of big crystals of mullite with a random distribution. The primary mullite has a long needle shape. The glassy matrix surrounded the smallest crystals of secondary mullite which are nucleated in the transitional liquid by dissolution of the alumina [16]. The grains of the secondary mullite present a different structure (acicular) and grains size smaller than that of the primary mullite. The structure of the sample MDD3 shows the presence of many pores with bigger dimensions.

The needle-like mullite grains observed for sample MDD3 treated at 1400 °C is larger than that observed for MDD1 sintered at the same temperature, this difference is caused by the high iron content in MDD3. According to Lecomte [28], the heat treatment at 1400 °C, performed on iron-enriched samples give rise to the formation of large needle-like mullite grains, widely separated from each other by a glassy phase. Also, the presence of iron oxide (Fe_2O_3) impurities contributes to reduce the liquid phase formation temperature. This promotes an increase in the alumina dissolution rate (Al_2O_3) in the liquid phase, in which Al ions react in higher proportions with Si ions [29]. According to the literature [29,30] in the clay minerals or mixtures of clay minerals, the alkalis, iron oxide (Fe_2O_3) and other impurities alter the composition of the liquid and its performance directly influences the recrystallization mechanisms. So, high alkaline oxide content favours crystal growth [30].

For the iron-rich kaolinic materials, at about 1400 °C, the interactions between the different phases in equilibrium lead to the formation of great amount of glassy phase. The iron compounds present in the samples may lead to the formation of eutectic liquids between 1300 and 1400 °C [28]. Indeed, this great amount of glassy phase is also related to other impurities. The presence of Na_2O_3 and K_2O promotes the formation of vitreous phase at a low melting point during the firing [31].

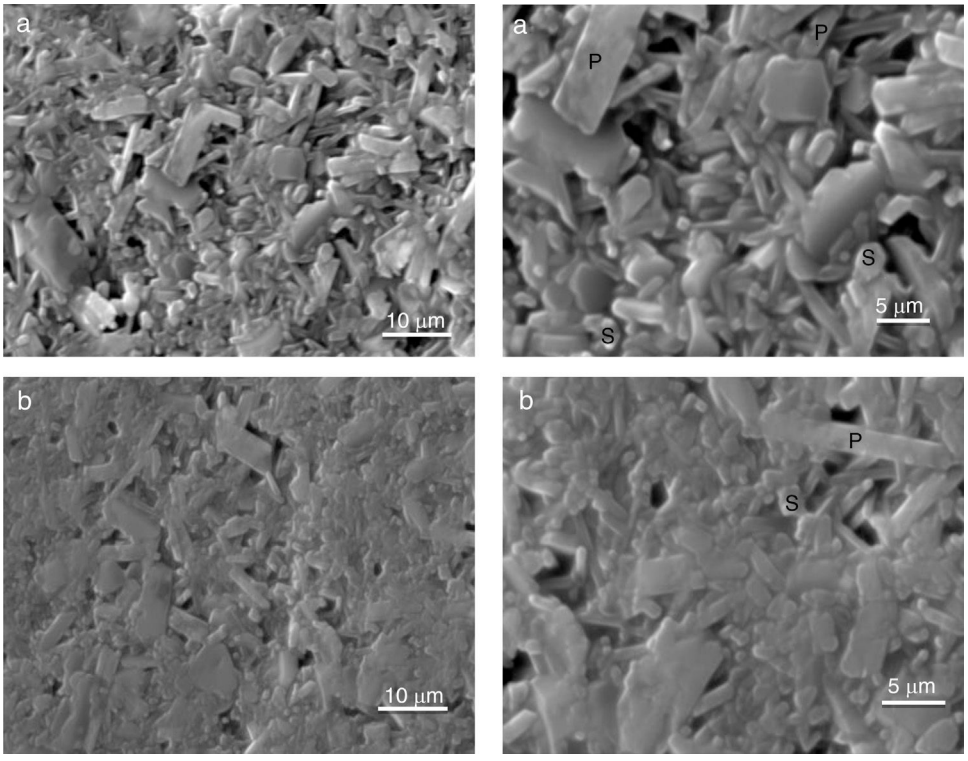

Fig. 11 – Microstructures obtained by SEM of the mixtures fired at 1400 °C during 2 h. (a) MDD3, (b) MDD1.

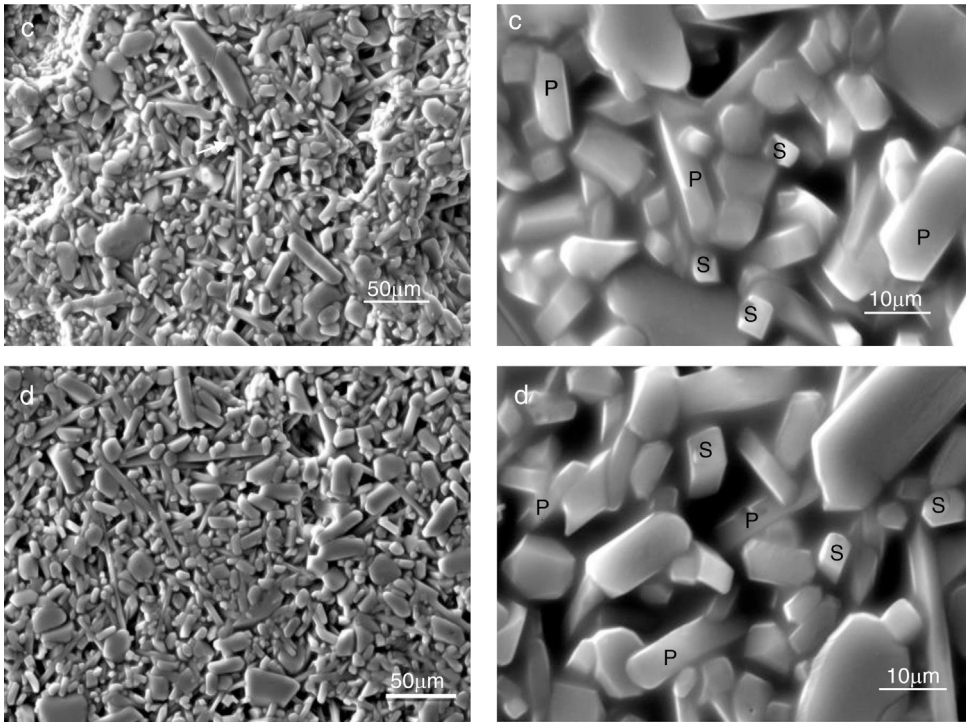

Fig. 12 – Microstructures obtained by SEM for mixtures fired at 1500 °C during 2 h. (c) MDD3, (d) MDD1, P: primary mullite, S: secondary mullite.

The firing at 1500 °C leads to a structure with a bimodal morphology. The size of the primary mullite crystals is bigger, compared to that obtained at 1400 °C. At high temperature, we observed a grains growth size of the mullite crystals and the formation of more secondary mullite crystals [16].

We know that mullite grains growth mechanism for high temperature in clays is a dissolution-precipitation process [32]. During heat treatment, dissolution rate of Al_2O_3 in to liquid phase increases, which promotes the mullite crystals growth [33].

At 1500 °C, the mullite grains size of crystals formed in MDD1 mixture is greater than that formed at MDD3 one. We explained this observation by the ratio Al_2O_3/SiO_2, which is equal for 1.45 to MDD1 and 1.22 for MDD3.

Conclusion

The obtained results show the possibility of using the aluminium slag as an addition (in replacement of α-alumina) for the elaboration of the mullite from kaolin. The curves of differential thermal analysis and thermo gravimetric analysis (DTA/TG) show that there are several phase transformations during firing. The microstructural analysis of samples sintered at 1500 °C shows the presence of the primary mullite in the form of lengthened needles and small crystals of secondary mullite, which are nucleated in the transient liquid. The transformation of the metakaolinite formed to the primary mullite, while the secondary mullite results from the reaction of the alumina of slag and from the excess of silica of the kaolin. Through this study, by reactive firing a dense mullite from natural kaolin and aluminium slag, this is an industrial obtained waste.

REFERENCES

[1] T. Huang, M.N. Rahaman, T.I. Mah, A. Triplicane, A. Parthasarathay, Anisotropic grain growth and microstructural evolution of dense mullite above 1550 °C, J. Am. Ceram. Soc. 83 (1) (2000) 204–210.
[2] M. Sardy, A. Arib, K. Abbassi, R. Moussa, M. Gomina, Elaboration and characterization of mullite refractory products from Moroccan andalusite, New J. Glass Ceram. 2 (2012) 121–125.
[3] I.A. Aksay, D.M. Dabbs, M. Sarikaya, Mullite for structural, electronic, and optical applications, J. Am. Ceram. Soc. 74 (10) (1991) 2341–2721.
[4] H.-J. Kleebe, F. Siegelin, T. Straubinger, G. Ziegler, Conversion of Al_2O_3–SiO_2 powder mixtures to 3:2 mullite following the stable or metastable phase diagram, J. Eur. Ceram. Soc. 21 (2001) 2521–2533.
[5] H. Rhanim, C. Olagnon, G. Fantozzi, R. Torrecillas, Experimental characterisation of high temperature creep resistance of mullite, Ceram. Int. 23 (6) (1997) 497–507.
[6] M. Hamidouche, N. Bouaouadja, C. Olagnon, G. Fantozzi, Thermal shock behaviour of mullite ceramic, Ceram. Int. 29 (2003) 599–609.
[7] T. Abdezadeh, Formation of mullite from precursor powders: sintering, microstructure and mechanical properties, Mater. Sci. Eng. A 355 (1–2) (2003) 56–61.
[8] L.B. Kong, T.S. Zhang, Y.Z. Chen, J. Ma, F. Boey, H. Huang, Microstructural composite mullite derived from oxides via a high-energy ball milling process, Ceram. Int. 30 (2004) 1313–1317.

[9] H.-J. Kleebe, F. Siegelin, T. Straubinger, G. Ziegler, Conversion of Al_2O_3–SiO_2 powder mixtures to 3:2 mullite following the stable or metastable phase diagram, J. Eur. Ceram. Soc. 21 (2001) 2521–25337.
[10] J. Roy, S. Maitra, Synthesis and characterization of sol–gel-derived chemical mullite, J. Ceram. Sci. Technol. 5 (01) (2014) 57–62.
[11] R. Septawendar, B.S. Purwasasmita, L. Nurdiwijayanto, A new synthesis route of nano mullite by calcining pulp precursors, J. Aust. Ceram. Soc. 47 (1) (2011) 42–47.
[12] M.A. Sainz, F.J. Serrano, J.M. Amigo b, J. Bastida, A. Caballero, XRD microstructural analysis of mullites obtained from kaolinite and alumina mixture, J. Eur. Ceram. Soc. 20 (2000) 403–412.
[13] L. Andrini, M.R. Gauna, M.S. Conconi, G. Suarez, F.G. Requejo, E.F. Agleitti, N.M. Rendtorff, Extended and local structural description of a kaolinitic clay, its fired ceramics and intermediates: an XRD and XANES analysis, J. Appl. Clay Sci. 124–125 (2016) 39–45.
[14] Y.-F. Chena, M.-C. Wang, M.H. Hona, Phase transformation and growth of mullite in kaolin ceramics, J. Eur. Ceram. Soc. 24 (2004) 2389–2397.
[15] M. Gonon, G. Fantozzi, H. Osmani, M. Hamidouche, M.A. Madjoubi, N. Bouaouadja, K. Loucif, Etude de la transformation de trois nuances de kaolin en fonction de la température, Silic. Ind. Cera. Sci. Tech. 65 (11–12) (2000) 119–124.
[16] T.J. Mackenzie, J.D. Schurcker, H. Schneider, J. Mcmanus, S. Wimperis, Phase evolution in mechanically treated mixtures of kaolinite and alumina hydrates (gibbsite and boehmite), J. Eur. Ceram. Soc. 20 (2000) 413–421.
[17] Y.F. Chen, M.C. Wang, M.H. Hon, Secondary mullite formation in kaolin–Al_2O_3 ceramics, J. Mater. Res. 18 (2003) 1355.
[18] M. Ohashi, Y. Iida, Hot forging of mullite-based ceramics prepared from kaolin-alumina, J. Am. Ceram. Soc. 83 (7) (2000) 1825–1827.
[19] J. Pascual, J. Zapatero, M.C. Jimenez de Haro, I. Varona, A. Justo, J.L. Perez-Rodriguez, P.J. Sanchez-Soto, Porous mullite and mullite-based composites by chemical processing of kaolinite and aluminum metal wastes, J. Mater. Chem. 10 (2000) 1409–1414.
[20] H. Belhouchet, M. Hamidouche, N. Bouaouadja, V. Garnier, G. Fantozzi, Crystallization kinetics of α-alumina and mullite-zirconia in boehmite and zircon mixture, J. Mater. Sci. Eng. A 3 (12) (2013) 814–819.
[21] H. Belhouchet, M. Hamidouche, N. Bouaouadja, V. Garnier, G. Fantozzi, Elaboration and characterization of mullite-zirconia composites from gibbsite, boehmite and zircon, J. Ceram. Silik. 53 (3) (2009) 205–210.
[22] H. Belhouchet, M. Hamidouche, R. Torrecillas, G. Fantozzi, The non-isothermal kinetics of mullite formation in boehmite–zircon mixtures, J. Therm. Anal. Calorim. 116 (2014) 795–803.
[23] H. Belhouchet, H. Makri, M. Hamidouche, N. Bouaouadja, V. Garnier, G. Fantozzi, Elaboration and characterization of multiphase composites obtained by reaction sintering of boehmite and zircon, J. Aust. Ceram. Soc. 50 (2) (2014) 135–146.
[24] S. Lamouri, M. Hamidouche, N. Bouaouadja, H. Belhouchet, V. Garnier, G. Fantozzi, J.F. Trelkat, Control of the γ-alumina to α-alumina phase transformation for an optimized alumina densification, Bol. Soc. Esp. Cerám. Vidrio 56 (2) (2017) 47–54.
[25] V. Viswabaskaran, F.D. Gnanam, M. Balasubramanian, Effect of MgO, Y_2O_3 and boehmite additives on the sintering behavior of mullite formed from kaolinite-reactive alumina, J. Mater. Process. Technol. 142 (2003) 275–281.
[26] P.G. Wherllyson, V.J. Silva, R.R. Menezes, G.A. Neves, H.L. Lira, L.N.L. Santana, Microstructural, physical and mechanical behavior of pastes containing clays and alumina waste, J. Appl. Clay Sci. 137 (2017) 259–265.
[27] C.J. McConville, W.E. Lee, Microstructural development on firing illite and smectite clays compared with that in kaolinite, J. Am. Ceram. Soc. 88 (2005) 2267–2276.
[28] G. Lecomte-Nana, J.P. Bonnet, N. Soro, Influence of iron on the occurrence of primary mullite in kaolin based materials: a semi-quantitative X-ray diffraction study, J. Eur. Ceram. Soc. 33 (2013) 669–677.
[29] V.J. Silva, M.F. Silva, W.P. Gonçalves, R.R. de Menezes, G.A. Neves, H.L. Lira, L.N.L. Santana, Porous mullite blocks with compositions containing kaolin and alumina waste, Ceram. Int. 42 (2016) 15471–15478.
[30] S. Deniel, N.T. Doyen, C. Dublanche-Tixier, D. Chateigner, P. Blanchart, Processing and characterization of textured mullite ceramics from phyllosilicates, J. Am. Chem. Soc. 30 (2010) 2427–2434.
[31] A. Arib, A. Sarhiri, R. Moussa, T. Remmal, M. Gomina, Caractéristiques structurales et mécaniques de céramiques à base d'argiles: Influence de la source de feldspath, C. R. Chim. 10 (2007) 502–510.
[32] H.P. Fang, M.H. Huang, Z.H. Chen, K. Xu, Y.G. Liu, Y.G. Huang, Effect of La_2O_3 additives on the strength and microstructure of mullite ceramics obtained from coal gangue and γ-Al_2O_3, Ceram. Int. 39 (2013) 6841–6846.
[33] X. Xu, X. Lao, J. Wu, Y. Zhang, X. Xu, K. Li, Microstructural evolution, phase transformations, and variations in physical properties of coal series kaolin powder compact during firing, Appl. Clay Sci. 115 (2015) 76–86.